AMD-Vol. 118

MECHANICS OF COMPOSITES AT ELEVATED AND CRYOGENIC TEMPERATURES

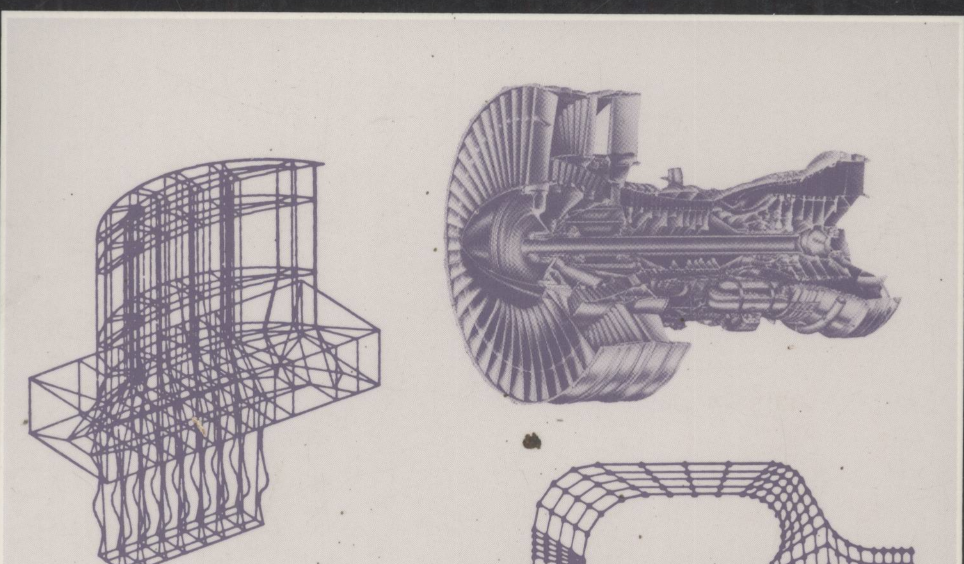

edited by

S. N. SINGHAL

W. F. JONES

C. T. HERAKOVICH

AMD-Vol. 118

MECHANICS OF COMPOSITES AT ELEVATED AND CRYOGENIC TEMPERATURES

PRESENTED AT
THE ASME APPLIED MECHANICS CONFERENCE
COLUMBUS, OHIO
JUNE 16–19, 1991

SPONSORED BY
THE APPLIED MECHANICS DIVISION, ASME

EDITED BY
S. N. SINGHAL
SVERDRUP TECHNOLOGY, INC.

W. F. JONES
OAK RIDGE NATIONAL LABORATORY

C. T. HERAKOVICH
UNIVERSITY OF VIRGINIA

THE AMERICAN SOCIETY OF MECHANICAL ENGINEERS
345 East 47th Street ■ United Engineering Center ■ New York, N.Y. 10017

Statement from By-Laws: The Society shall not be responsible for statements or opinions advanced in papers ... or printed in its publications (7.1.3)

ISBN No. 0-7918-0724-X

Library of Congress
Catalog Number 91-55354

FOREWORD

This volume contains 24 peer-reviewed papers which were presented at the symposium on "Mechanics of Composites at Elevated and Cryogenic Temperatures," which was held in June of 1991 at The Ohio State University in Columbus, Ohio. The Symposium was sponsored by the Committee on Composite Materials of the Applied Mechanics Division, ASME, and was held at the 1991 Applied Mechanics Division Meeting. This Symposium was one of many that the Committee organizes every year for presentation at various Division meetings.

The Symposium brought together leading researchers in the field of composite materials for elevated and cryogenic temperatures, who discussed their work in six technical sessions and a panel discussion on Current and Future Directions of High Temperature Composite Structures.

The panel discussion was organized and chaired by C. C. Chamis of NASA Lewis Research Center. Technical session topics included Modeling of Thermal Stresses, Micromechanical Characterization, Thermal Fracture and Fatigue, Creep and Inelastic Behavior, and Dynamics and Buckling Analysis. Many of the authors also served as chairpersons during the symposium. The editors wish to thank all of the authors, chairpersons, and panelists who participated in the symposium. Thanks are also given to the authors and reviewers who helped with the publication of this volume.

S. N. Singhal
W. F. Jones
C. T. Herakovich
Symposium Co-Chairmen

CONTENTS

AMD-Vol. 118, Mechanics of Composites at
Elevated and Cryogenic Temperatures
ASME 1991

THERMO-MECHANICAL RESPONSE PREDICTIONS FOR METAL MATRIX COMPOSITE LAMINATES

J. Aboudi[1], J. S. Hidde[2], and C. T. Herakovich
University of Virginia
Charlottesville, Virginia

ABSTRACT

An analytical, micromechanical model is employed for prediction of the stress-strain response of metal matrix composite laminates subjected to thermo-mechanical loading. The predicted behavior of laminates is based upon knowledge of the thermo-mechanical response of the transversely isotropic, elastic fibers and the elastic-viscoplastic, work-hardening matrix.

The method is applied to study the behavior of silicon carbide/titanium metal matrix composite laminates. The response of laminates is compared with that of unidirectional lamina. The results demonstrate the effect of cooling from a stress-free temperature and the mismatch of thermal and mechanical properties of the constituent phases on the laminate's subsequent mechanical response. Typical results are presented for a variety of laminates subjected to monotonic tension, monotonic shear and cyclic tensile/compressive loadings.

INTRODUCTION

As engineers and scientists strive to improve the performance of structures and materials for applications in extreme environments, it is natural that their attention has turned to metal matrix fibrous composite materials. Metal matrix composites (MMC) offer a broad range of potential advantages depending upon the application. Some of the most important advantages include high stiffness, high strength, dimensional stability, fatigue resistance, and lower weight. The choice of fiber and matrix usually depends upon the load requirements, environmental conditions, and cost.

A significant advantage of metal matrix composites is the ability to use them at elevated temperatures where resin matrices decompose and burn. Consequently, modeling the inelastic behavior of MMC unidirectional laminae and laminates is of a significant importance to the technical community. Several available elastic-plastic models of fibrous composite materials can be found in the review article by Bahei-El-Din and Dvorak (1989). More recent works on MMC include those by Bahei-El-Din (1990), Fujita et al (1990), Dvorak et al (1991) and Sun et al (1990).

The method of cells is a micromechanical model of periodic array of fibers which was recently reviewed by Aboudi (1989). This micromechanical approach is analytical and requires minimal computational effort while offering the ability to predict the behavior of composites under a wide variety of thermomechanical loading conditions.

The prediction of thermo-mechanical yield surfaces of metal matrix lamina was presented previously by Herakovich et al (1990). In the present paper the micromechanical method is generalized for the prediction of the nonlinear, thermo-mechanical response of laminates. This extension enables the study of the effect of the mismatch of thermal expansion properties of the fiber and matrix phases upon cooling from a stress-free temperature on a laminate's subsequent stress-strain response.

---

[1]Visiting from Tel Aviv University, Tel Aviv, Israel

[2]Now with Michelin Americas Research & Development, Greenville, S.C.

Thus the residual stresses induced in the matrix material due to a temperature change can be accounted for in the micromechanical predictions and used in the prediction of laminate response.

The laminate exhibits an additional level of sophistication over the lamina. In addition to the micromechanical mismatch effects, there are the effects of mismatch in effective properties of different layers in a laminate. Further, individual layers of the laminate may "yield" at different thermo-mechanical load states and this must be modeled when predicting the effective nonlinear stress-strain response of the laminate.

In the following, typical results are presented for monotonic tension, monotonic shear, and cyclic tensile/compressive thermo-mechanical loadings of unidirectional lamina and laminates.

FORMULATION

As mentioned previously, the micromechanical method of cells was reviewed in Aboudi (1989). The method models a unidirectional fibrous composite as a repeating fiber cell imbedded regularly in the matrix (Fig. 1a). The fibers have a square cross section h_1^2 and are arranged at a distance h_2 apart. A typical representative cell (Fig. 1b) consists of a fiber subcell and three matrix subcells. The micromechanics analysis of the representative cell consists of the application of the continuity of displacements and tractions at the interfaces between the subcells and between neighboring cells on an average basis together with equilibrium considerations.

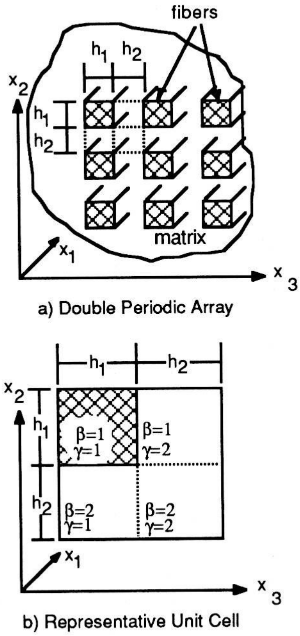

Fig. 1. Method of cells model

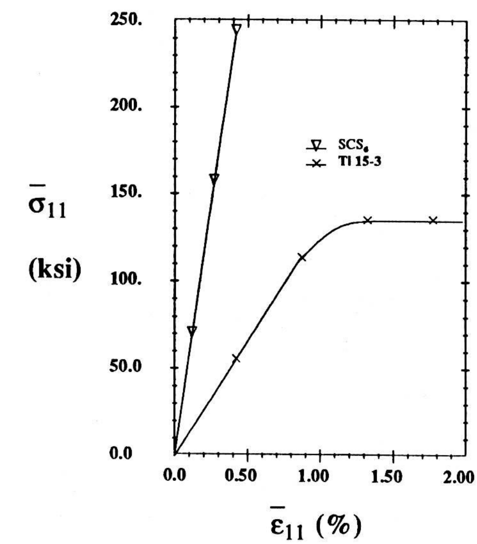

Fig. 2. Constituent Responses

Consider an inelastic metal matrix reinforced by unidirectional fibers. The matrix is assumed to be an isotropic elastic-viscoplastic material. Its viscoplastic behavior is described by the Bodner and Partom (1975) unified theory of plasticity. Thus, the constitutive laws governing the matrix material behavior can be expressed in the form

$$\sigma^{(m)} = C^{(m)}(\varepsilon^{(m)} - \varepsilon^{PL\,(m)}) - \Gamma^{(m)}\Delta T \tag{1}$$

The plastic strain rate of the viscoplastic material is given by

$$\dot{\varepsilon}^{PL(m)} = \Lambda_m \hat{\sigma}^{(m)} \tag{2}$$

where $\hat{\sigma}^{(m)}$ is the deviatoric stress tensor.

In (2), Λ_m is the flow rule function which is given, according to Bodner and Partom unified theory by

$$\Lambda_m = D_0 \exp\left\{-\hat{n}\left[Z^2/(3J_2)\right]^n\right\}/J_2^{1/2} \tag{3}$$

with $\hat{n} = 0.5(n+1)/n$, $J_2 = \hat{\sigma}_{ij}\hat{\sigma}_{ij}/2$, and D_0 and n being inelastic parameters. In (3) Z is a state variable which in the case of isotropic hardening can be determined from

$$Z = Z_1 + (Z_0 - Z_1) \exp\left[-m\, W_P/Z_0\right]$$

where W_P is the plastic work, and Z_0, Z_1, m are additional plastic parameters.

The fibers are considered to be elastic and transversely isotropic, i.e.,

$$\boldsymbol{\sigma}^{(f)} = \mathbf{C}^{(f)}\boldsymbol{\varepsilon}^{(f)} - \boldsymbol{\Gamma}^{(f)}\Delta T \tag{4}$$

where $\mathbf{C}^{(f)}$ and $\boldsymbol{\Gamma}^{(f)}$ are the corresponding quantities which describe the fiber material behavior.

It can be shown (Aboudi, 1989) that the micromechanics analysis leads to the following constitutive law which controls the overall behavior of the unidirectional metal matrix composite

$$\bar{\boldsymbol{\sigma}} = \mathbf{E}(\bar{\boldsymbol{\varepsilon}} - \bar{\boldsymbol{\varepsilon}}^{PL}) - \mathbf{U}\Delta T \tag{5}$$

Here, $\bar{\boldsymbol{\sigma}}$ and $\bar{\boldsymbol{\varepsilon}}$ denote the average stresses and strains in the composite, $\bar{\boldsymbol{\varepsilon}}^{PL}$ is the average plastic strain, **E** is the effective stiffness matrix and **U** ΔT represents the thermal term in which ΔT is the deviation of the temperature from a reference temperature at which the material is stress-free and the elastic strain is zero. The explicit form of the elements of **E** and **U** in terms of the fiber and matrix properties and reinforcement ratio can be found in Aboudi (1989), where the evolution law of $\bar{\boldsymbol{\varepsilon}}^{PL}$ is also given.

The constitutive law (5) can be employed to predict the nonlinear behavior of unidirectional fibrous composites from the knowledge of the material properties of the constituents. By utilizing the classical lamination theory one can establish the following constitutive equations of metal matrix composite laminates.

$$\begin{bmatrix}\mathbf{N}\\ \mathbf{M}\end{bmatrix} = \begin{bmatrix}\mathbf{A} & \mathbf{B}\\ \mathbf{B} & \mathbf{D}\end{bmatrix}\begin{bmatrix}\boldsymbol{\varepsilon}^0\\ \boldsymbol{\kappa}\end{bmatrix} - \begin{bmatrix}\mathbf{N}^{PL}\\ \mathbf{M}^{PL}\end{bmatrix} - \begin{bmatrix}\mathbf{N}^{T}\\ \mathbf{M}^{T}\end{bmatrix} \tag{6}$$

In eqn. (6), **N** and **M** denote the stress resultant and moments, and $\boldsymbol{\varepsilon}^0$, $\boldsymbol{\kappa}$ are the laminate midplane strains and curvatures. The terms $\mathbf{N}^{PL}$, $\mathbf{M}^{PL}$ denote plastic resultants and moments, and $\mathbf{N}^T$, $\mathbf{M}^T$ correspond to the thermal resultants and moments. Finally, **A**, **B** and **D** are the extensional stiffness matrix, the coupling stiffness matrix, and bending stiffness matrix, respectively. Note that while eqn. (5) is formulated in terms of material coordinate system (x_1, x_2, x_3) in which the fibers are oriented in the x_1 direction, eqn. (6) is given in terms of the laminate coordinate system (x, y, z) in which z is normal to the middle surface.

TYPICAL RESULTS

The derived constitutive relations which govern the response of metal matrix laminates are employed herein to predict the nonlinear response of continuous SCS_6 silicon carbide fiber, Ti-15-3 titanium matrix composites. All laminates investigated had a symmetric stacking sequence. Stress-strain response predictions were determined for the stress-free residual state ($\Delta T = 0$) and for thermo-mechanical loadings in which the temperature was decreased (corresponding to a fabrication process) followed by mechanical loading. In this analysis, all material properties were considered temperature independent. The material properties assumed for each constituent material are presented in Table 1 and the stress-strain curves for the two constituents are presented in Fig. 2. As indicated in the figure, the fiber is linear elastic and the matrix is elastic, nearly perfectly plastic with a maximum stress of approximately 135 ksi. A fiber volume fraction $v_f = 0.4$ was chosen for all predictions of composite response.

Unidirectional Lamina

The thermo-mechanical stress-strain responses for four different load histories are shown in Fig. 3. The four curves correspond to temperature changes of 0, -1000, -3000, and -5000° F followed by mechanical loading $\varepsilon_{11} = 2.0\%$. The axial contraction with zero average stress under the thermal loading and subsequent nonlinear response under mechanical loading are clearly evident in the figure for all four load histories. It was determined in Herakovich et al (1990) that initial yielding of a subcell occurred at a temperature change of -4230° F for pure thermal loading. Thus the response for $\Delta T = -5000$ includes yielding during the thermal loading. A temperature change of -5000° F is not realistic for SCS_6/Ti-15-3 as the material cannot withstand the high temperatures required for such a temperature change. Nevertheless, the predictions are presented to demonstrate the effects of thermal yielding followed by mechanical loading for MMC.

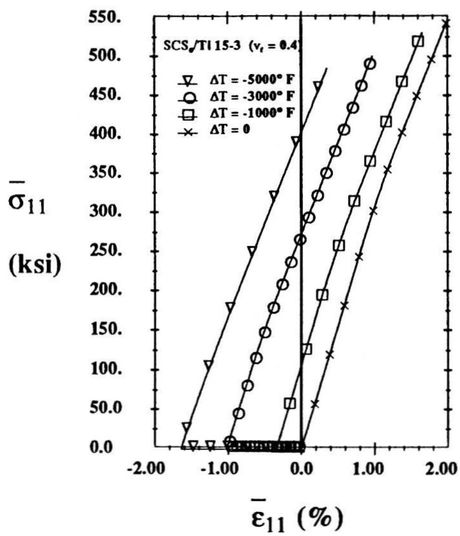

Fig. 3. Thermo-mechanical $\bar{\sigma}_{11}$ vs $\bar{\varepsilon}_{11}$

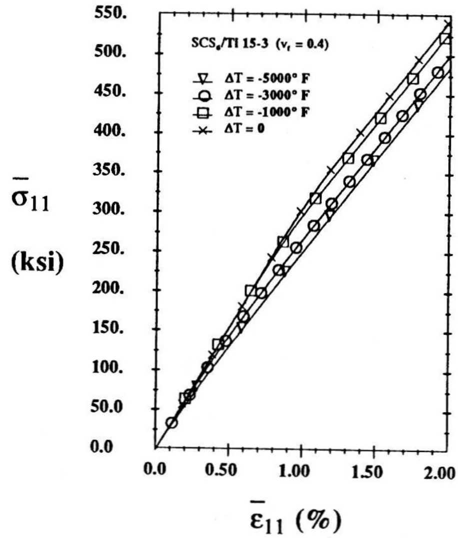

Fig. 4. Mechanical $\bar{\sigma}_{11}$ vs $\bar{\varepsilon}_{11}$

The effects of the residual thermal stresses on the axial stress-strain response for the different thermal loadings is demonstrated more clearly in Fig. 4. In this figure the curves have been shifted such that the mechanical loadings all initiate at the origin. The figure clearly shows a monotonically decreasing proportional limit with increasing magnitude of ΔT. The stiffness of the response after complete yielding of the matrix is identical for all four load cases as exhibited by the parallel final slopes of the stress-strain curves. The final stiffness corresponds very closely to the rule of mixtures prediction with zero contribution from the matrix.

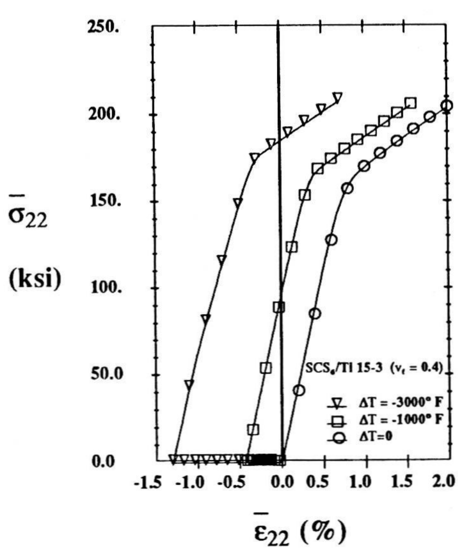

Fig. 5. Thermo-mechanical $\bar{\sigma}_{22}$ vs $\bar{\varepsilon}_{22}$

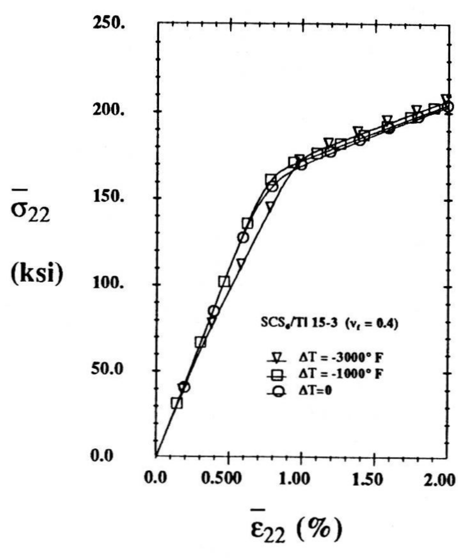

Fig. 6. Mechanical $\bar{\sigma}_{22}$ vs $\bar{\varepsilon}_{22}$

Table 1. MATERIAL PROPERTIES OF SCS_6 FIBERS AND TI-15-3 MATRIX

SCS_6	E_A(Msi)$^+$	ν_A	E_T(Msi)	ν_T
	58.0	0.25	58.0	0.25
	G_A(Msi)	Y (ksi)	$\alpha_A(10^{-6}/°F)$	$\alpha_T(10^{-6}/°F)$
	23.2	---	2.77	2.57
Ti-15-3	E(Msi)	ν	G(Msi)	n
	13.2	0.36	4.83	7.0
	D_0 (sec)	Z_0 (ksi)	Z_1 (ksi)	m
	10^4	140	170	1700
	Y (ksi)	$\alpha(10^{-6}/°F)$		
	110	5.14		

+ (subscripts A and T denote axial and transverse directions)

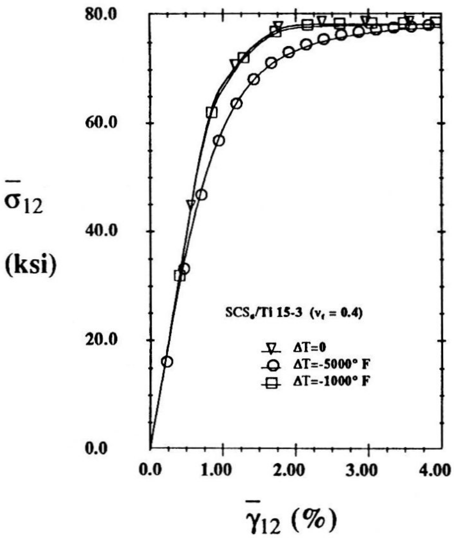

Fig. 7. Mechanical $\bar{\sigma}_{12}$ vs $\bar{\gamma}_{12}$

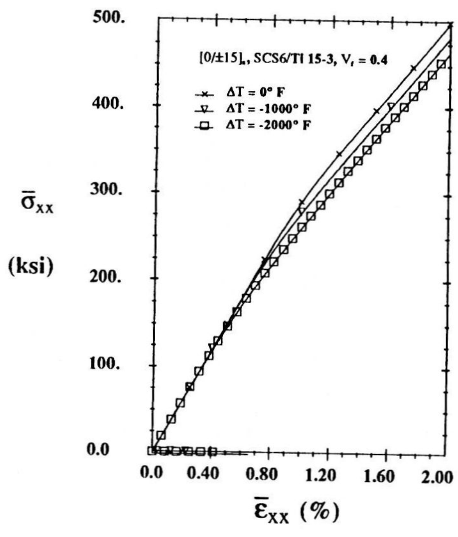

Fig. 8. Mechanical $\bar{\sigma}_{xx}$ vs $\bar{\varepsilon}_{xx}$ - [0/±15]$_s$

Transverse responses for three thermal-mechanical loadings are shown in Figs. 5 & 6. It is evident from Fig. 5 that the transverse response under mechanical loading exhibits a much sharper nonlinearity than does the axial response. This is expected since the transverse response is more of a matrix dominated response. The results in Fig. 6 where the mechanical responses have been shifted to initiate at the origin exhibit some surprising results. The proportional limit is not a monotonic function of the temperature change. The proportional limit for ΔT = -1000° F is higher than that for ΔT = 0, but that for ΔT = -3000° F is lower than for ΔT = 0. Also, while initial yielding at low stress levels is evident for ΔT = -3000° F, complete yielding at this temperature occurs at a higher final stress than the lower ΔT cases. Indeed, after complete yielding of the matrix, the stress-strain curves are in the order of the temperature changes with the largest temperature change corresponding to the most "strain-hardening". To be sure, the changes with thermal loading are relatively small, but nevertheless evident.

The inplane shear response of the unidirectional lamina for three different thermal loading conditions is shown in Fig. 7. The proportional limit in shear decreases with increasing ΔT with all curves attaining approximately the same fully yielded shear stress.

These results for the thermo-mechanical response of unidirectional laminae (Figs. 3-7) demonstrate the tri-axial nature of the residual stress state. Subsequent yielding due to mechanical loading is dependent on the type of mechanical loading and the degree of thermal loading.

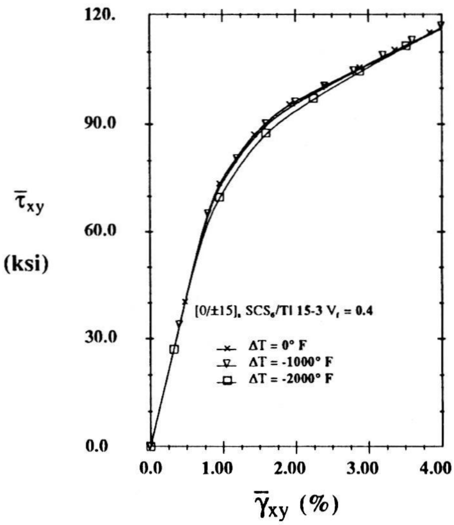

Fig. 9. Mechanical $\bar{\sigma}_{xx}$ vs $\bar{\varepsilon}_{xx}$ – $[0/\pm15]_s$

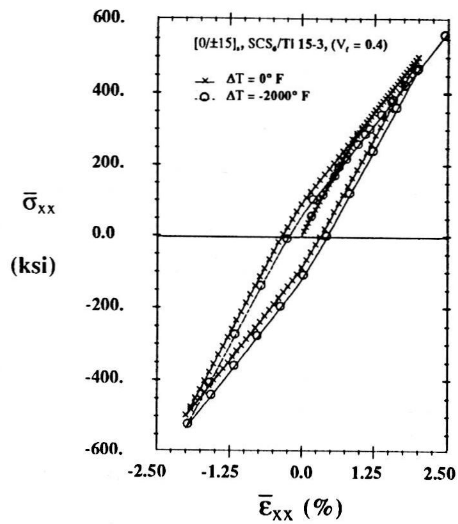

Fig. 10. Cyclic Mechanical $\bar{\sigma}_{xx}$ vs $\bar{\varepsilon}_{xx}$ – $[0/\pm15]_s$

LAMINATES

Three different laminates have been chosen to demonstrate the nonlinear thermo-mechanical response of laminated MMC, and the versatility of the method of cells. The presented results are typical of results for a larger number of laminates which were studied during the course of the investigation. Additional results are not presented due to space limitations and the lack of any significant differences in response. In all of the following laminate results, the curves have been shifted such that the mechanical loading initiates from the origin.

Figure 8 shows the tensile response of a $[0/\pm15]_s$ laminate for three different thermal conditions. Clearly the proportional limit decreases monotonically with increasing magnitude of temperature change and the final stiffness is the same for all three thermal conditions. The shear response for this same laminate is shown in Fig. 9. These results show that the shear response is affected very little by the residual thermal stresses. Comparison of the axial responses (Fig. 8) and shear responses (Fig. 9) indicates that residual stresses have more influence on the axial response than on the shear response.

Cyclic tensile-compressive thermo-mechanical loading of a $[0/\pm15]_s$ laminate is shown for two thermal conditions in Fig. 10. As in the previous results for this laminate, the residual stresses do not affect significantly the overall response either for the loading or unloading mechanical phases. The thermal stresses have the effect of translating the stress-strain response without significantly altering the size or shape of the curves. One difference in the curves is the lower initial proportional limit in the presence of thermal stresses. These results clearly demonstrate the ability of the model to track completely the thermo-mechanical, cyclic response of the laminates.

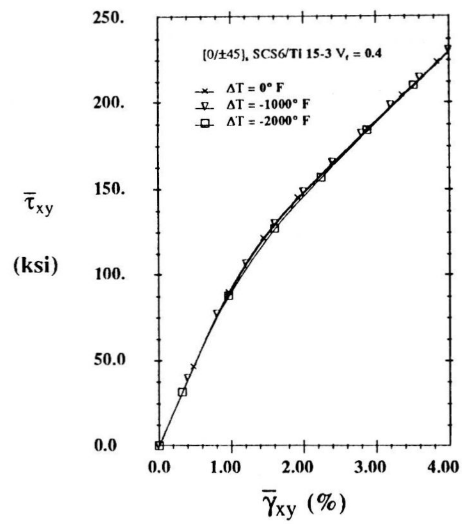

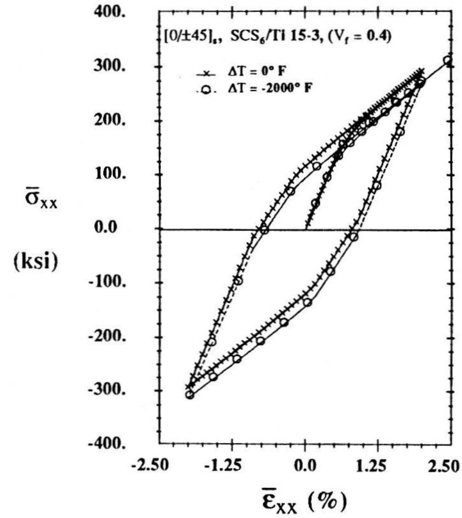

Fig. 11. Mechanical $\bar{\tau}_{xy}$ vs $\bar{\gamma}_{xy}$ - $[0/\pm45]_s$

Fig. 12. Cyclic Mechanical $\bar{\sigma}_{xx}$ vs $\bar{\varepsilon}_{xx}$ - $[0/\pm45]_s$

The shear response of a $[0/\pm45]_s$ laminate is shown in Fig. 11 for three different thermal conditions. The shear response is almost identical for all three conditions. The cyclic tensile-compressive response of this laminate for two thermal states is shown in Fig. 12. Comparison of these results with those of Fig. 10 for the $[0/\pm15]_s$ laminate indicates the expected lower yield stress and greater ductility for the $[0/\pm45]_s$ laminate. Otherwise the responses are quite similar with the thermal stresses again shifting the response but not otherwise altering its size or shape. The results in Fig. 12 show clearly the different linear segments of the stress-strain response corresponding to "yielding" of the different layers of the laminate.

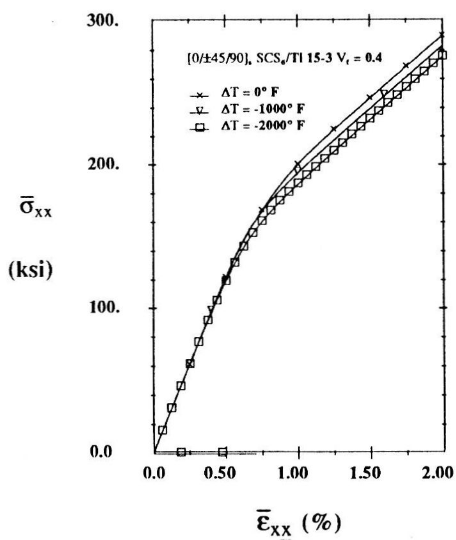

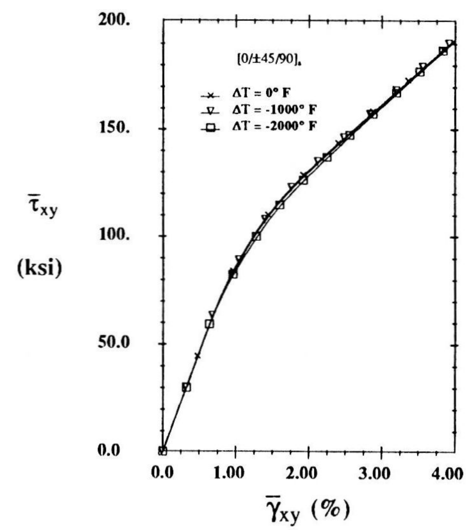

Fig. 13. Mechanical $\bar{\sigma}_{xx}$ vs $\bar{\varepsilon}_{xx}$ - $[0/\pm45/90]_s$

Fig. 14. Mechanical $\bar{\tau}_{xy}$ vs $\bar{\gamma}_{xy}$ - $[0/\pm45/90]_s$

The final laminate to be considered is the $[0/\pm45/90]_s$. The axial response (Fig. 13) and the shear response (Fig. 14) for three thermal-mechanical load conditions exhibit the same type of response that was exhibited by the other laminates. The proportional limit for axial response decreases with increasing temperature change, but the shear response is affected only minimally by residual stresses.

CONCLUSIONS

The method of cells has been shown to be very versatile for predicting the thermo-mechanical response of laminated composites. It has been shown that thermal stresses do not have a major influence on either the axial or shear response of laminates. The primary effect of thermal stresses in laminates is a relatively small shift in the stress-strain response. It has also been shown that the effects of thermal stresses is more significant in unidirectional lamina than in laminates.

ACKNOWLEDGEMENT

This work was supported by the General Electric Company (200-14-14Y05751), the Virginia Center for Innovative Technology (CAE-89-006), NASA Langley Research Center (NAG 1-745), and the Center for Light Thermal Structures at the University of Virginia. The authors are grateful for this support.

REFERENCES

Aboudi, J., 1989, "Micromechanical Analysis of Composites by the Method of Cells," *Applied Mechanics Review*, Vol. 42, pp. 193-221.

Bahei-El-Din, R. S. Shah and Dvorak, G. J., 1989, "A Review of Plasticity Theory of Fibrous Composite Materials", *Metal Matrix Composites: Testing, Analysis, and Failure Modes ASTM STP 1032*, W.S.Johnson, ed., American Society Testing & Materials, Philadelphia, pp. 103-129.

Bahei-El-Din, R. S. Shah, 1990, "Plasticity Analysis of Fibrous Laminates Under Thermomechanical Loads", *Thermal and Mechanical Behavior of Metal matrix and Ceramic Matrix Composites, ASTM STP 1080*, J. M. Kennedy, H. H. Moeller, and W. S. Johnson, eds., American Society Testing & Materials, Philadelphia, pp. 20-39.

Bodner, S. R. and Partom, Y., 1975, "Constitutive Equations for Elastic-viscoplastic Strain Hardening Materials", *Journal Applied Mechanics*, Vol. 42, pp. 385-389.

Dvorak, G. J., Bahei-El-Din, R. S. Shah & Nigam, H., 1991, "Experiments and Modeling in Plasticity of Fibrous Composites", *Inelastic Deformation of Composite Materials*, G. J. Dvorak, ed., Springer-Verlag, New York, pp. 283-309.

Fujita, T., Pindera, M-J, Herakovich, C. T., 1990, "Temperature-Dependent Tensile and Shear Response of P100/6061 Graphite-Aluminum", *Thermal and Mechanical Behavior of Metal Matrix and Ceramic Matrix Composites, ASTM STP 1080*, J. M. Kennedy, H. H. Moeller, and W. S. Johnson, eds., American Society Testing & Materials, Philadelphia, pp. 165-182.

Herakovich, C. T., Aboudi, J. and Beuth, J. L., Jr., 1990, "A Micromechanical Composite Yield Model Accounting for Residual Stresses", *Inelastic Deformation of Composite Materials*, G. J.Dvorak, ed., Springer-Verlag, New York, pp. 373-388.

Sun, C. T., Chen, J. L., Sha, G. T., and Koop, W. E., 1990, "Mechanical Characterization of SCS-6/Ti-6-4 Metal Matrix Composite", *Journal Composite Materials*, Vol 24, pp. 1029-1059.

AMD-Vol. 118, Mechanics of Composites at
Elevated and Cryogenic Temperatures
ASME 1991

A THERMOMECHANICAL ANALYSIS OF LAMINATED METAL MATRIX COMPOSITES USING THE VISCOPLASTICITY THEORY BASED ON OVERSTRESS

Nan-Ming Yeh and Erhard Krempl
Mechanics of Materials Laboratory
Rensselaer Polytechnic Institute
Troy, New York

ABSTRACT

The vanishing fiber diameter model (VFD) and the thermoviscoplasticity theory based on overstress (TVBO) are used to analyse the thermo–mechanical behavior of angle–ply composite laminates using classical laminate theory. TVBO is a "unified" theory which does not separately postulate constitutive equations for creep and rate–independent plasticity. All inelastic deformation is considered rate–dependent and the concept of a yield surface is not used.

Assuming that fiber and matrix are stress free at the manufacturing temperature and remain perfectly bonded during cool down to room temperature the model permits the calculation of residual stresses between fiber and matrix which can influence the subsequent thermomechanical deformation behavior. A time–dependent, slowly diminishing redistribution of the residual stresses is predicted while the composite is sitting stress free at room temperature. As a consequence subsequent mechanical behavior depends on time spent at room temperature until the stress redistribution is complete which for the chosen material properties happens to occur after 30 days. Tension/compression asymmetry for a unidirectional and a $(\pm 12^o)_S$ B/Al laminate are two examples for which detailed numerical analyses are performed. The results are encouraging and reflect the trends of the few available experimental results.

INTRODUCTION

Future airplanes and space structures need to be made of materials with high specific strength and stiffness as well as high fatigue and fracture resistance. Metal matrix composites are prime candidates for these applications. When thermal and mechanical cycling is involved as is frequently the case, stresses between fiber and matrix may develop when a mismatch of the coefficients of thermal expansion of matrix and fiber is present. These internal stresses may affect the mechanical behavior of the composite and may lead to premature failure. It is therefore necessary to develop analysis tools to predict and alleviate these internal stresses in the design stage. Since rate (time)–dependent effects are frequently present a thermoviscoplastic analysis is in order.

In an early experimental investigation Cheskis and Heckel [1970] used X–ray techniques to measure fiber and matrix stresses in a 2024 Al/W composite. They showed that the yield behavior of the composites is significantly influenced by manufacturing residual stresses.

Dvorak and Rao [1976] used a plasticity theory to compute the residual stresses in heat–treated metal matrix composites. They concluded that the residual stresses found after heat–treatment are significant in magnitude and a high hydrostatic stress component in the matrix at the fiber–matrix interface may cause fracture or fatigue damage.

The purpose of this paper is to present a simple tool to analyze the thermomechanical behavior of metal matrix composite laminates for time dependent deformation including rate sensitivity, relaxation and creep. To this end the thermoviscoplasticity theory (TVBO) of Lee and Krempl [1991] is combined with the vanishing fiber diameter model (VFD) of Dvorak and Bahei–El–Din [1982] to determine the plane stress behavior of angle–ply laminates using standard classical laminate theory. Of special interest are the influences of fabrication residual stresses on the mechanical behavior. The residual stresses which develop during cool–down from manufacturing temperature and which can redistribute with time while the composite is stress free at room temperature are found to have a significant influence on the room temperature tension/compression behavior. The TVBO theory used here represents viscoplastic behavior which is sometimes called "cold creep", i.e. the creep behavior in metals seen at low homologous temperature. The growth laws for the state variables must be augmented by a suitable recovery of state term to represent secondary creep in the quasi elastic region of the stress–strain diagram. Such modifications are easily implemented but are not pursued here due to the lack of high temperature composite creep data.

THE COMPOSITE MODEL. THERMOVISCOPLASTICITY THEORY BASED ON OVERSTRESS (TVBO) AND THE VANISHING FIBER DIAMETER MODEL (VFD)

The Governing Equations

The three dimensional thermoviscoplasticity theory based on overstress has been developed by Lee and Krempl [1991]. In the present analysis a plane stress state in a fibrous ply is assumed. The usual vector notation for the stress tensor components σ and the small strain tensor components ϵ are used for the representation of the equations. Boldface capital letters denote 3x3 matrices.

Stresses and strains without a superscript designate quantities imposed on the composite as a whole. Superscripts ^{f} and ^{m} denote fiber and matrix, respectively. The fiber volume fraction is c^f and c^m denotes the matrix volume fraction with $c^f + c^m = 1$. The fiber is transversely isotropic thermoelastic, the matrix is isotropic, inelastically incompressible and thermoviscoplastic as represented by TVBO. Fiber orientation in the x–direction is postulated, see Fig. 1. The x y s is the preferred or on–axis coordinate system and 1 2 6 is the off–axis system. For convenience in writing we denote the vectors which are referred to be the off–axis system with a prime.

For the VFD model, Dvorak and Bahei–El–Din [1982], the following constraint equations hold

$$\begin{aligned} \dot{\sigma}_i &= \dot{\sigma}_i^f = \dot{\sigma}_i^m \quad \text{for } i = y, s \\ \dot{\sigma}_x &= c^f \dot{\sigma}_x^f + c^m \dot{\sigma}_x^m \\ \dot{\epsilon}_i &= c^f \dot{\epsilon}_i^f + c^m \dot{\epsilon}_i^m \quad \text{for } i = y, s \\ \dot{\epsilon}_x &= \dot{\epsilon}_x^f = \dot{\epsilon}_x^m. \end{aligned} \tag{1}$$

When they are combined with the TVBO equations by Lee and Krempl [1991] the composite is characterized by the following set of equations: (details can be found in Yeh and Krempl [1990])

$$\dot{\epsilon} = \overline{\mathbf{C}}^{-1}\dot{\sigma} + (\mathbf{K}^m)^{-1}\mathbf{X}^m + (\dot{\mathbf{R}}^f)^{-1}\sigma^f + (\dot{\mathbf{R}}^m)^{-1}\sigma^m + \overline{\alpha}\dot{T} \tag{2}$$

together with a separate growth law for the σ_x^m component of the matrix

$$\dot{\sigma}_x^m = \frac{E^m}{E_{xx}}\dot{\sigma}_x - \frac{c^f}{E_{xx}} L\dot{\sigma}_y - \frac{c^f E_{xx}^f E^m}{E_{xx}}\left[\frac{1}{K^m k^m[\Gamma^m]}(x_x^m - 0.5x_y^m)\right]$$
$$-\frac{c^f E_{xx}^f E^m}{E_{xx}}\left\{\left[\frac{1}{(E_{xx}^f)^2}(\dot{\nu}_{xy}^f E_{xx}^f - \nu_{xy}^f \dot{E}_{xx}^f) - \frac{1}{(E^m)^2}(\dot{\nu}^m E^m - \nu^m \dot{E}^m)\right]\sigma_y\right.$$
$$\left. + \frac{\dot{E}_{xx}^f}{(E_{xx}^f)^2}\sigma_x^f - \frac{\dot{E}^m}{(E^m)^2}\sigma_x^m\right\} - \frac{c^f E_{xx}^f E^m}{E_{xx}}(\alpha^m - \alpha_x^f)\dot{T}. \quad (3)$$

In addition growth laws for the two state variables of TVBO, the matrix equilibrium stress $\mathbf{g}^m$ and the kinematic stress $\mathbf{f}^m$, are given as

$$\dot{\mathbf{g}}^m = q^m[\Gamma^m]\dot{\boldsymbol{\sigma}}^m + \dot{T}\,\frac{\partial q^m[\Gamma^m]}{\partial T}\boldsymbol{\sigma}^m + \left\{q^m[\Gamma^m] - \theta^m\left[q^m[\Gamma^m] - p^m(1-q^m[\Gamma^m])\right]\right\}\frac{\mathbf{x}^m}{k^m[\Gamma^m]} \quad (4)$$

and

$$\dot{\mathbf{f}}^m = \frac{p^m}{k^m[\Gamma^m]}\mathbf{x}^m, \quad (5)$$

respectively, with

$$(\Gamma^m)^2 = (\mathbf{x}^m)^t\,\mathbf{H}\,(\mathbf{x}^m)$$

$$(\theta^m)^2 = \frac{1}{(A^m)^2}(\mathbf{z}^m)^t\,\mathbf{H}\,(\mathbf{z}^m)$$

$$\mathbf{x}^m = \boldsymbol{\sigma}^m - \mathbf{g}^m$$

$$\mathbf{z}^m = \mathbf{g}^m - \mathbf{f}^m$$

$$\mathbf{H} = \begin{bmatrix} 1 & -0.5 & 0 \\ -0.5 & 1 & 0 \\ 0 & 0 & 3 \end{bmatrix} \quad (6)$$

In the above inelastic incompressibility for the matrix is assumed. $\bar{\mathbf{C}}^{-1}$ is the overall compliance matrix and $(\mathbf{K}^m)^{-1}$ is the viscosity matrix. The matrices $(\dot{\mathbf{R}}^f)^{-1}$ and $(\dot{\mathbf{R}}^m)^{-1}$ contain time derivatives of the elastic constants of the fiber and the matrix, respectively. All components of these four matrices are listed in Appendix I. The viscosity function $k^m[\Gamma^m]$ and the dimensionless shape function $q^m[\Gamma^m]$ are decreasing ($q^m[0] < 1$ is required, see Lee and Krempl [1991]) and control the rate dependence and the shape of the stress–strain diagram, respectively. (Square brackets following a symbol denote "function of".) The quantity p^m represents the ratio of the tangent modulus E_t^m at the maximum inelastic strain of interest to the viscosity factor K^m. It sets the slope of stress–inelastic strain diagram at the maximum strain of interest. E_{xx}, L, $\bar{\boldsymbol{\alpha}}$ are defined in Appendix I. An explanation of TVBO is given by Lee and Krempl [1991].

Eq. (3) is used to calculate the instantaneous axial matrix stress which can not be obtained from the overall boundary conditions directly. σ_x^m is affected by mechanical and thermal loadings and their loading paths. For instance for pure thermal loading (overall